The origin and formation model of Permian dolostones on the northwestern margin of Junggar Basin, China

Xinchuan Lu *, Ji'an Shi, Shuncun Zhang, Niuniu Zou, Guoqiang Sun, Shengyin Zhang

Key Laboratory of Petroleum Resources Research, Gansu Province/Key Laboratory of Petroleum Resources Research, Institute of Geology and Geophysics, Chinese Academy of Sciences, Lanzhou 730000, PR China

A B S T R A C T

This study investigates the mechanism of dolostone formation and establishes a dolomitization model in the Permian strata on the northwestern margin of Junggar Basin, China. Dolomitic rock samples are collected from the Permian Fengcheng Formation in Urho area and then characterized by petrological, mineralogical, carbon and oxygen isotope, and trace element geochemical analyses. Results show that the major types of dolomitic rocks include dolomitic mudstone, dolomitic siltstone, dolomitized tuffaceous siltstone, and dolomitized tuffaceous mudstone. The dolomitized rocks are dominated by euhedral or subhedral powder- and fine-crystal dolomites formed by replacement lacustrine argilla-calcareous and siliceous (tuffaceous) components and commonly filled with residual and late calcite cements. The parameters of dolomitic rocks show great variations, including the V/Ni ratio (1.02–4.88), Sr content (95.9–783.6 µg/g), Mg/Ca ratio (0.68–5.13), degree of ordering (0.39–1.00), $\delta^{18}O_{PDB}$ (−14.8‰ to 3.2‰), and $\delta^{13}C_{PDB}$ (−1‰ to 5.2‰). The dolomitic rocks have multi-stage origins and were formed in a semi-closed continental brackish-saltwater bay with weak hydrodynamic processes, deep water bodies, and relatively quiet conditions. In the Permian depositional stage, a combination of complex tectonic activities, fault development, hot subtropical climate, and frequent volcanic activities provided not only Mg^{2+} source for dolomitization but also channels for rapid flow and seepage of Mg-rich fluids. The origins of dolostones in the study area include penecontemporaneous dolomitization, burial dolomitization, and hydrothermal dolomitization. This study lays a foundation for further studies on dolomite formation and dolomite reservoir, and provides effective methods for researching complex dolostone (tuffaceous, shale and silty dolomite) formation.

1. Introduction

Carbonate rocks are among the most widely distributed sedimentary rocks on Earth, which account for 20–25% of total sedimentary rocks in the geological history (Sam, 2001). Fifty percent of the world's total oil and gas reserves (60% of total oil and gas production) comes from carbonate rock reservoirs, of which more than half present in dolostone reservoirs (Zenger et al., 1980; Roehl and Choquette, 1985). Weyl (1960) and Zhang et al. (2011) consider that the process of dolomitization must proceed via mole-for-mole exchange of calcium by magnesium without macrotransport of carbonate; the porosity of the rock is not only affected by 13% volume shrinkage in the process, allowing dolomitic formation easily to become reservoir. In North America and the Middle and Far East, even up to 80% of carbonate rock reservoirs

are composed of dolostones or transformed by dolomitization (Roehl and Choquette, 1985; Warren, 2000).

Dolomite reservoirs are so important. Previous studies on dolomites have mainly been focused on marine, lacustrine, and argillaceous or sandstone-associated dolostones (He et al., 2005; Tian et al., 2000; Zhang, 1993; Fan et al., 2003; Zhang et al., 2011). Dolomite formation is affected by many factors. The major styles of dolomite include Sabkha- and Coorong-style dolomite (Friedman and Sanders, 1967; Hsu and Schneider, 1973), evaporitic reflux dolomite (Adams and Rhodes, 1960; Warren, 1999), mixing zone (of seawater and meteoric water) dolomite (Hanshow et al., 1971; Badiozamani, 1973; Muchez and Viaene, 1994; Fookes, 1995), burial dolomite (Gao et al., 1992, 1995; Qing and Mountjoy, 1994a,b), organogenic dolomite (Baker and Kastener, 1981), bacterial mediation dolomite (Gunatilaka et al., 1987; Li and Liu, 2013; Luo et al., 2013), and hydrothermal dolomite (Davies and Smith, 2006; Machel, 2004).

In China, massive dolostone reservoirs, mainly marine carbonate rock reservoirs, are found through oil and gas exploration. In

---

* Corresponding author.
 E-mail address: xclu@lzb.ac.cn (X. Lu).

Sichuan Basin, marine dolostone reservoirs are widely distributed from the old Sinian Dengying Formation in Hanyuan region in the southwest to the new oolitic dolomite formations in the Lower Triassic Feixianguan Formation (Luo et al., 1998; Ma, 1999; He et al., 2005). In Ordos Basin, marine dolostone reservoirs present in the Lower Ordovician Majiagou Formation (He et al., 2005). Continental dolostone reservoirs are widely distributed in the Permian strata in Junggar Basin; Paleogene strata in Kuqa Depressio, Tuotuo River in Qinghai Province, Biyang Sag in Nan-Xiang Basin, Qianjiang River in Jianghan Basin, Bohai Bay Basin, Liaodong Bay Basin, and Sanshui Basin in Guangdong Province; Cretaceous-Paleogene strata in Linhe Depression, Inner Mongolia; Lower Cretaceous strata in Jiuquan Basin and Erlian Basin; and Upper Cretaceous strata in Songliao Basin (Tian et al., 2000; Zhang, 1993). Many researchers have studied on the origin of those dolomite, and established some styles of dolomite formations. In short, dolomite formation is mainly burial dolostone, such as Ordovician dolomitic deposition in Ordos basin (Su et al., 2011; Chen et al., 2013) and Tarim basin (Zhang et al., 2008; Li et al., 2011). Penecontemporaneous and burial dolomite is the characteristic component of dolostone reservoir in the Permian Changxing Formation, Sichuan basin (Dang et al., 2011; Zheng et al., 2007). These dolomites are formed in the environment of limestone and sandsone. The comprehensive research suggests that there is less study on the Permian dolomite at present, correspondingly, the studies concentrating on the argillaceous and tuffaceous dolomite are rare.

In 2008, a set of dolomitized reservoirs with industrial oil flow was found in the Permian Fengcheng Formation on the northwestern margin of Junggar Basin. In recent years, exploration and development works in this area have proven that this set of dolomite formations are excellent hydrocarbon reservoirs and has huge reserves of oil and gas resources (Kuang et al., 2012). The major types of dolomitic rocks in these reservoirs are powder- and fine-crystal dolomite, argillaceous dolomite, tuffaceous dolomite, and dolomitic siltstone (Xue et al., 2012). Presently, research on the origin and formation mechanism of these dolomitic rocks is still in its early stage. Jiang et al. (2012), Xue et al. (2012), and Zhu et al. (2013) studied dolomite formation by considering various types and structures of dolostone. They think the dolomite formed evaporation, replacement, hydrothermal genesis, but those relatively complete lack of comprehensive analysis. Presently, in-depth studies are needed to further elucidate the characteristics and origin of dolomite.

In the present study, we focus on Permian dolostone reservoirs on northwestern margin of the Junggar Basin. The rock type, rock-forming environment, origin, and formation mechanism of dolomitic rock samples were examined using a combination of qualitative and quantitative methods. The results were discussed to identify the source of Magnesium-rich fluids and the relationship between water–rock interaction and dolomitization, further to establish a model of dolomitization in the study area. These will provide new thought for deployment strategy of oil and gas exploration in dolostone reservoirs in Junggar Basin as well as reference data for in-depth studies on dolomite formation.

2. Regional setting and stratigraphic division

The Urho-Fengcheng area is located in the lower reach of Jiamuhe River in the north part of Junggar's northwestern margin. This study area is 100 km southwest from Karamay City and belongs to the central north section of a foreland thrust belt on Junggar's northwestern margin (Fig. 1a). Deep faults are developed around which a number of parallel or oblique secondary faults are derived. The resulting fault terraces are approximately 16 km in width, which provide favorable conditions for hydrocarbon

migration and occlusion (Yang and Zhang, 2007; Geng and Chen, 2002; Guo et al., 2009; Qi and Wu, 2009).

Since the Late Paleozoic, Junggar Basin had experienced multi-stage tectonic events, including the Hercynian, Indosinian, Yanshanian, and Himalayan orogenies. Polycyclic structural development resulted in multi-stage tectonic activities and diverse structural combinations as well as sedimentary systems in the basin, which jointly controlled the processes of hydrocarbon generation, migration, accumulation, and dissipation. In the Permian depositional stage, there was mainly an alluvial fan or fan delta depositional environment under the influence of multi-stage volcanic activities.

In a previous study, Zhang et al. (2007) have divided the Permian strata into five formations, including (from bottom to top) the Lower Permian Jiamuhe (P_1j, approx. 540 m) and Fengcheng Formation of strata (P_1f, approx. 390 m), the Middle Permian Xiazijie (P_2x, approx. 480 m) and Lower Urho Formation (P_2w, approx. 660 m), and the Upper Permian Upper Urho Formation (P_3w, approx. 270 m). The Permian strata are 2000–2500 m thick and massively deposited in Mahu Sag (Fig. 1b).

The present study was conducted on dolostones of the Lower Permian Fengcheng Formation, including members 1 (P_1f^1), 2 (P_1f^2), and 3 (P_1f^3). These members are mainly composed of volcanic rock and tuffaceous dolomite (P_1f^1); argillaceous dolomite (P_1f^2); and argillaceous dolomite and siltstone (P_1f^3). P_1f mainly consists of lacustrine deposits, with P_1f^1 experiencing frequent volcanic activities, P_1f^2 dominated by dolomitic rocks, and P_1f^3 dominated by dolomitic mudstone and sandstone (Fig. 2).

The study area should be a semi-closed continental salinity lacustrine sedimentary environment in the lower Permian Series Fengcheng Formation (Liu, 1989; Zhang et al., 2007). There are fan-delta front, shore, shallow, semi-deep lake, and eruptive subfacies from land to lake. The deposits of fan-delta front underwater distributary channel and sheet sand microfacies mainly consist of gray-yellow sandstone. The deposits of shore, shallow, semi-deep lake subfacies are made up of silty sand and clay. The eruptive subfacies sediments consist of tuff. The dolomite mainly lies in fan-delta front subfacies sheet sand microfacies, shallow, semi-deep lake subfacies, and eruptive subfacies (Fig. 2).

3. Materials and methods

This study involved sedimentological, petrological, mineralogical, isotopic (carbon and oxygen), and trace element geochemical analyses of rock samples collected form 9 wells (Fig. 1). Petrographic characteristics were corroborated by coring, thin sectioning, scan electronic microscopy and X-ray diffraction (XRD) analysis of 32 cores samples from the 9 wells.

For stable-isotope analysis, microsamples (from 34 samples of 7 cores) were prepared as powders drilled from cut surfaces corresponding to the areas that had been thin-sectioned. Carbonate powders were reacted with 100% phosphoric acid (density >1.9, Wachter and Hayes, 1985) at 90 °C using a Kiel III online carbonate preparation line connected to a ThermoFinnigan 252 mass spectrometer. All values are reported in per mil relative to V-PDB by assigning a $\delta^{13}C$ value of +1.95‰ and a $\delta^{18}O$ value of −2.20‰ to NBS19. Reproducibility was checked by replicate analysis of laboratory standards and is better than ±0.04‰ (carbon) and 0.07‰ (oxygen) (1σ).

Major/trace elements analysis was completed using a 3080E3X X-ray fluorospectrometer in the Key Laboratory of Petroleum Resources Research, Institute of Geology and Geophysics, Chinese Academy of Sciences, Lanzhou, China.

To obtain more detailed textural information, dolostone surfaces of microsamples (from 27 samples of 6 cores) were studied
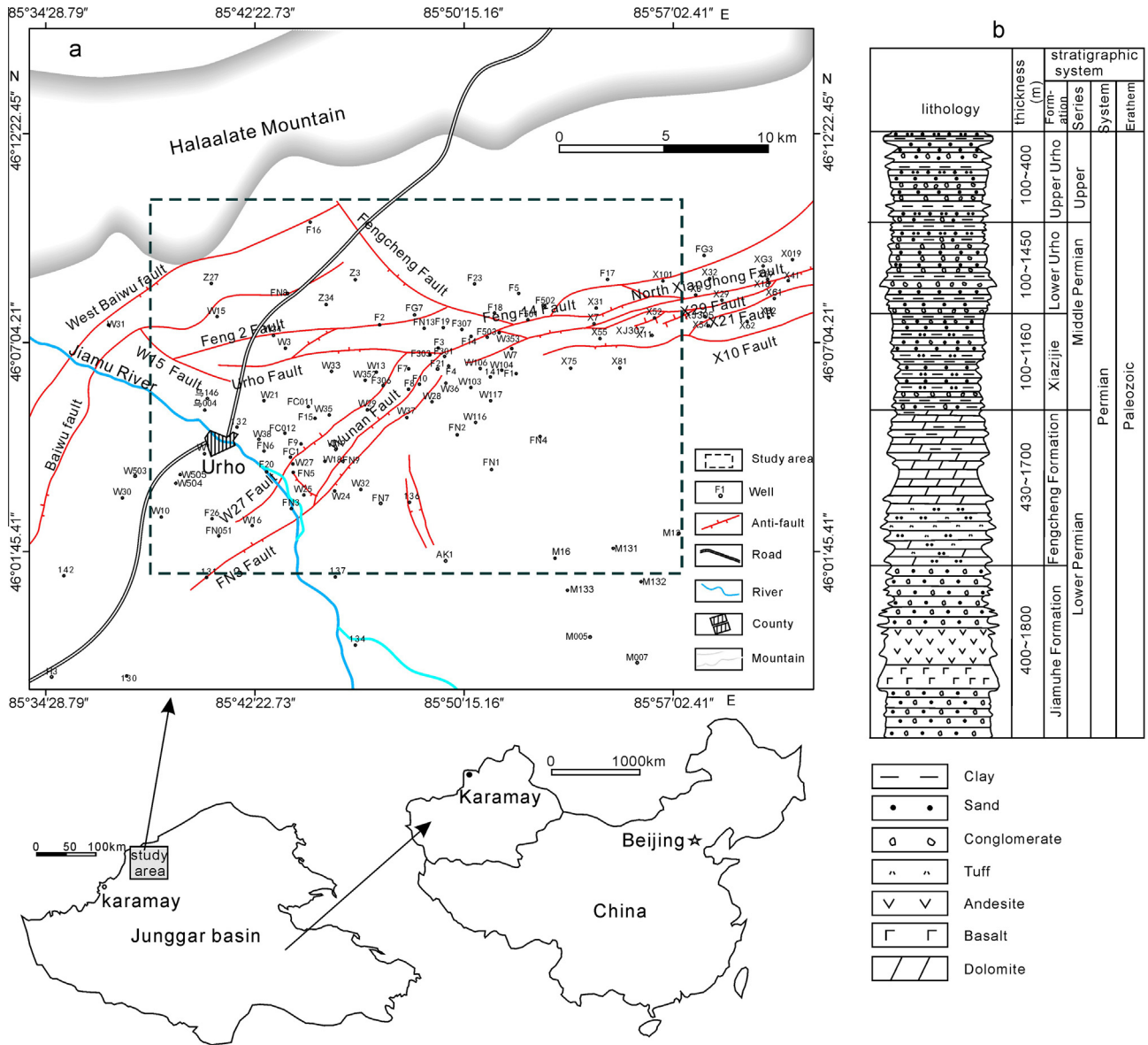
Fig. 1. The location and tectonic characteristics of the study area, and the Permian coloumn for Northweast Junggar basin.

using a JSM-5600 scanning electron microscope in the State Key Laboratory of Solid Lubrication, Lanzhou Institute of Chemical Physics, Chinese Academy of Sciences, Lanzhou, China.

XRD analysis was carried out with powdered bulk rock materials on a Dmax 12KW powder X-ray diffractometer (Micro Structure Analytical Laboratory, Beijing University Science Park, Beijing, China) using Fefiltered Co Kα radiation. The samples were step-scanned at 4–70° 2θ interval. In part of them (without quartz and/or anhydrite content) metal silicon was used as internal standard. The d-spacing of the dolomite peak (104) and the relative intensities of the (015) and (110) peaks (computed as integral intensities) were measured on the XRD patterns.

4. Results

4.1. Petrographic characteristics of dolomite

Macro- and micro-structures of cores and thin sections show that dolomitic rocks in the Permian Fengcheng Formation are dominated by argillaceous and tuffaceous dolostone followed by silty dolostone. That is, dolostones mainly present in mudstone, tuff, and siltstone in the study area (Fig. 3). In these dolostones, dolomites are mainly micritic and micro-crystal dolomites in uneven distribution and developed along textures, fissure fillings, fractures, and beddings, mostly in strip, laminated, or massive patterns (Fig. 3). The dolomite crystals are euhedral to a low degree, mainly in subhedral shapes with a small amount in euhedral shapes. Specifically, powder-crystal, micro-crystal, and micritic dolomites are euhedral to a less extent and mainly in subhedral shapes; fine- and medium-crystal dolomites are euhedral to a more extent and generally in euhedral shapes (Fig. 3). Except for dolomitized rocks, the rock matrix mainly comprises tuffaceous mudstone, calcareous mudstone, or siliceous mudstone (Fig. 3b–g).

In the Lower Permian P₁f, dolostone-associated rocks of have complex lithologic features. A major unique feature is that dolomitized rocks present in tuff, which increases the difficulty in studying dolostones in the study area. The morphology and composition of dolostones in tuff were characterized using scanning electron microscopy and electron microprobe. In terms
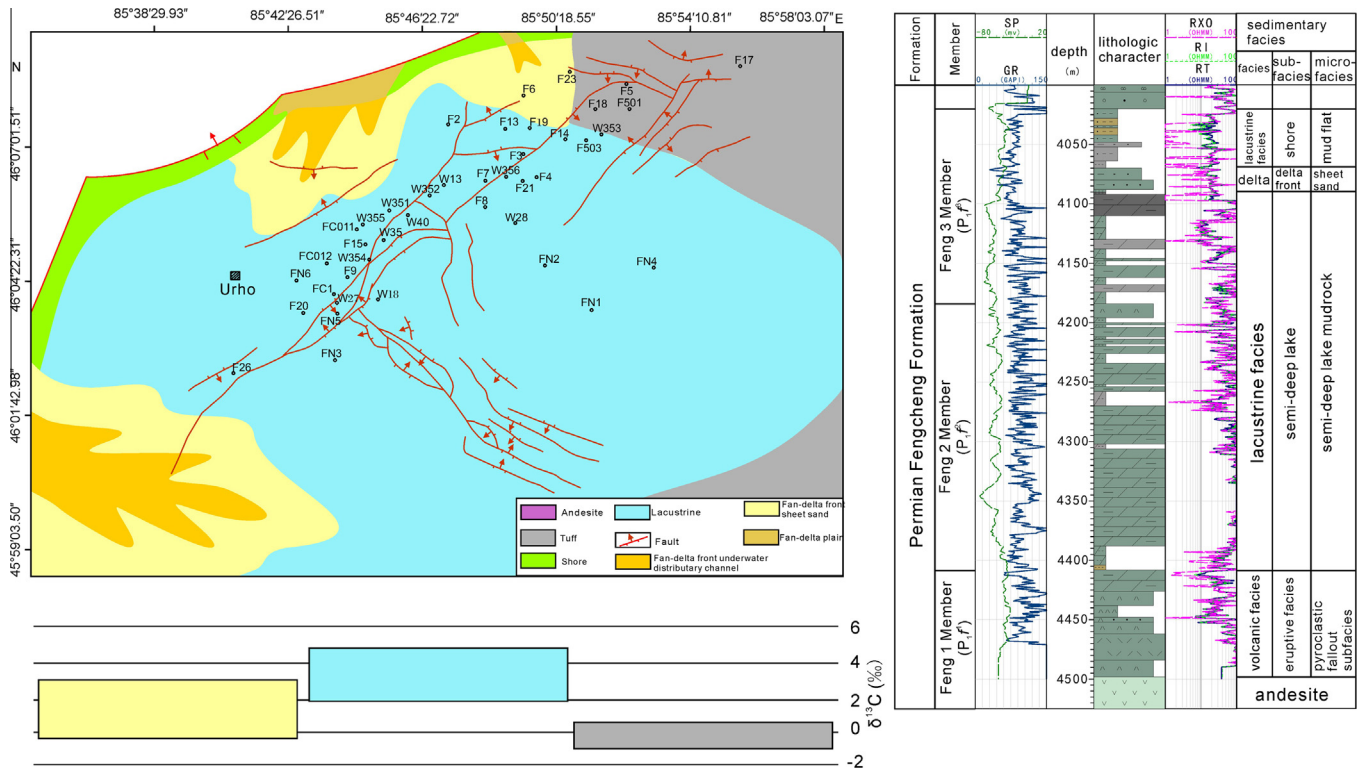
Fig. 2. The sedimentary facies map of Fengcheng 2 Formation in study area, and a composite columnar section of single well (FN1).

of surface morphology, there exists authigenic dolomite in the tight tuff; energy spectra show that the tuff (point A) contains relatively more Si, K, and Fe with less Mg while the dolostone (point B) contains relatively more Ca and Mg with less Si (Fig. 3d, Table 1).

4.2. Degree of order in dolomite

The degree of order in dolostones is the ratio between the intensity values of the (015) to (110) diffraction peaks. Results show that the degree of order in dolostones ranges from 0.39 to 1.00 with an average of 0.60 (Table 2).

4.3. Carbon and oxygen isotope values and trace element contents

In our study area, the V/Ni ratio of dolostone samples falls in the range of 1.02–4.88 with Ni content substantially varying in the range of 6.5–99.9 μg/g. Only three samples contain >40 μg/g Ni, whereas the vast majority of rock samples contain <40 μg/g Ni (Table 2). Strontium content of dolomitic rock samples significantly varies in the range of 95.9–783.6 μg/g (Table 2).

The $\delta^{18}O_{PDB}$ values of dolomitic rock samples range from the minimum −14.8‰ to the maximum 3.2‰, with an average of 2.94‰; the $\delta^{13}C_{PDB}$ values range from −1‰ to 5.2‰, with an average of 2.98‰ (Table 2).

5. Discussion

5.1. Crystal morphology and structure of dolostone-forming

The characteristics of dolomite crystals are closely related to their formation environment. Thus, studies often consider the characteristics of dolomite crystal structure to identify the dolomite-forming environment (Braithwaite et al., 2004; Wang et al., 2010). In the thin sections of rock samples from the Lower Permian Series Fengcheng Formation, dolomites present in micritic

to medium crystals and euhedral to subhedral forms. According to the above characteristics of dolomite crystal structure and combined with the crystal form identification criteria of Wang et al. (2010), we propose that the origins of dolostone in the Lower Permian Fengcheng Formation is complex: micritic and powder-crystal dolostones may be penecontemporaneous dolostones (Fig. 3b and g); the euhedral–subhedral crystal structures are of burial dolostones, mainly the shallow burial type (Fig. 3d and e); and the crystal contact surfaces are in irregular shapes, with point, surface, and curved surface contact related to medium burial type and hydrothermal fluids. Dolomite filling fractures were observed in cores and thin sections, providing strong evidence for the occurrence of hydrothermal dolostones (Fig. 3c and f).

In the study area, Dolomicrite and tuff are interbedded with deposits of gypsum rock, commonly showing wavy laminae, dolomicrite structure, horizontal bedding, and drain structure (Fig. 3b and g), which characteristics of dolomites are direct reflections of penecontemporaneous dolomitization.

In the depositional stage of Permian P_1f, there existed intense volcanic activities. As driven by hydrothermal flows generated from volcanic eruption, high-pressure high-temperatures Magnesium-rich fluids infiltrated to the overlying formations or migrated upward along faults, forming the hydrothermal dolomite. Such hydrothermal dolomites are often syndiagenetic to saline minerals such as borosilicate sodalite, albite, barite, analcime, and shortite (Kuang et al., 2012). Of these, borosilicate sodalite (Fig. 3h), analcime, and shortite commonly present in this study area. Owing to the hydrothermal activity in the late Fengcheng Formation in Wuxia area, there exist vein-like calcite and dolomite distributed along fractures (Fig. 3c). Despite a lack of typical hydrothermal saddle dolomite, we found a small amount of ankerite, providing an evidence for the hydrothermal origin.

Additionally, Junggar Basin experienced increasingly intensive collisions in the peripheral areas during the Late Carboniferous-Early Permian, and the resulting formation of nappe on the
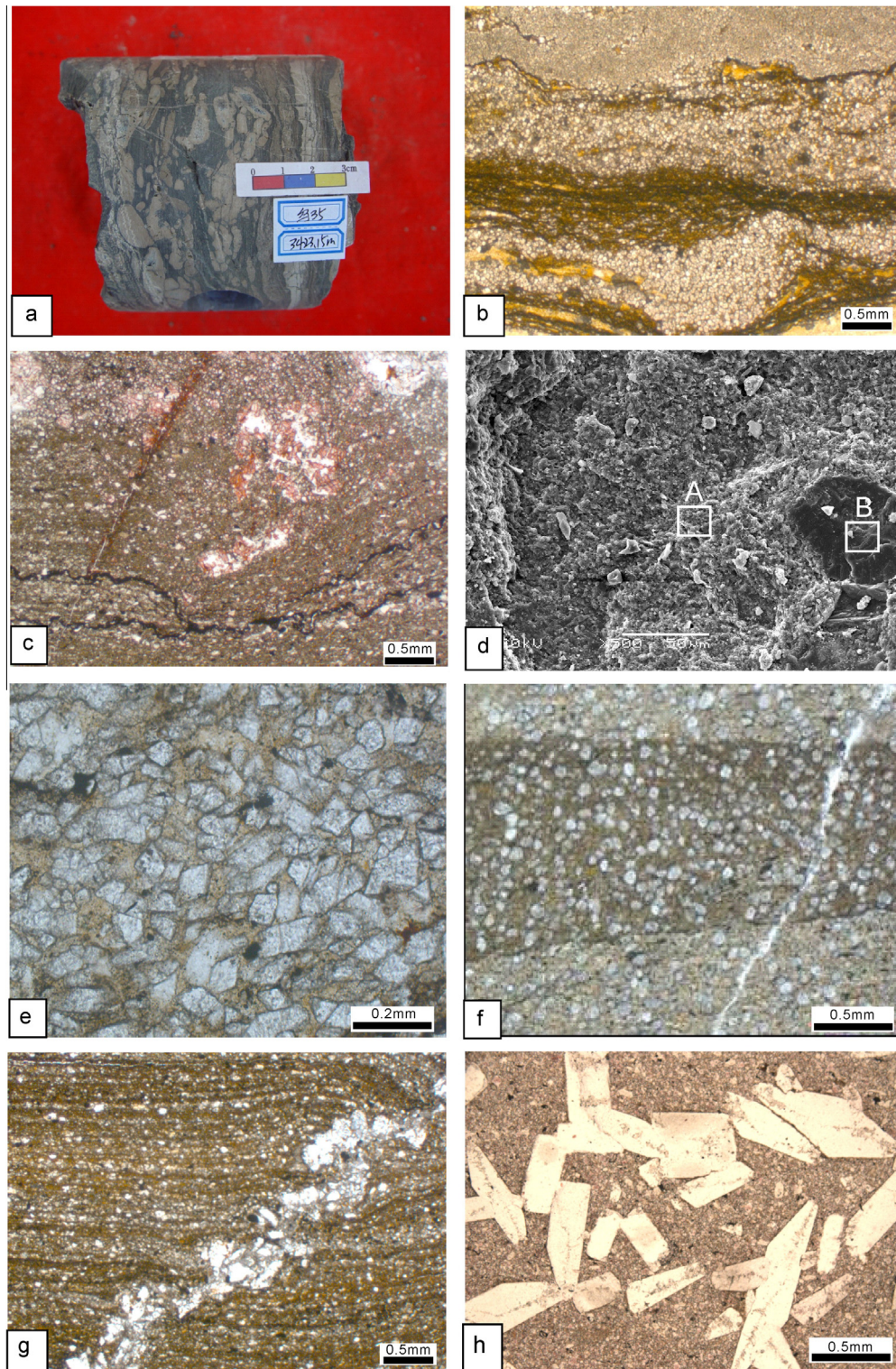
Fig. 3. macroscopic and microscopic characteristics of dolomitic rocks in the Permian Fengcheng Formation in the study area. (a) Well W35, 3423.15 m, P_1f^3, bedding and massive structures in argillaceous dolostone; (b) well W35, 3421.79 m, P_1f^3, microstructure of argillaceous dolostone formed by dolomitization; (c) well F6, 3466.80 m, P_1f^3, incomplete dolomitization in tuffaceous mudstone, with residual calcite; (d) well FN1, 4275.0 m, P_1f^2, microstructure of dolomitic tuff, with tuff as the matrix (A) and cine-crystal dolomites in subhedral and anhedral forms (B); (e) well F3, 3245.0 m, P_1f^3, microstructure of the subhedral form in argillaceous fine-crystal dolostone; and (f) well F5, 3250.95 m, P_1f^2, star-like distribution of subhedral dolomite in argillaceous dolostone, with fractures filled with hydrothermal dolostone; (g) well F7, 3193.5 m, P_1f^3, cine-crystal dolomites in tuffaceous mudstone; (h) well FN3, 4129.6 m, P_1f^2, euhedral borosilicate sodalite in tuffaceous domomite.

northwestern margin provided a structural basis for the development of fractures. Burial dolomitization is often closely related to the development of fractures and stylolite. In the study area, syndiagenetic overthrust activity of Wuxia Fault accelerated the upwelling of deep Magnesium-rich fluids as well as their rapid infiltration and flow across the formations. Fractures or faults developed along tectonic activities further transformed sediments rich in calcium carbonate, leading to the formation of burial type

Table 1
Energy spectrum data of points A (left) and B (right) in Fig. 3d.

A						B					
Element	Line	Weight%	K-ratio	Cnts/s	Atomic%	Element	Line	Weight%	K-ratio	Cnts/s	Atomic%
Mg	Ka	0.77	0.0049	3.64	1.01	Mg	Ka	5.75	0.0272	18.63	9.04
Al	Ka	5.07	0.0382	30.49	5.99	Al	Ka	0.64	0.0036	2.62	0.91
Si	Ka	57.72	0.4634	373.17	65.61	Si	Ka	3.08	0.0216	16	4.19
Cl	Ka	1.58	0.0105	7.38	1.42	Cl	Ka	0.96	0.0089	5.8	1.04
K	Ka	21.45	0.1699	103.33	17.51	K	Ka	1.33	0.0147	8.25	1.3
Ca	Ka	2.56	0.0198	11.09	2.04	Ca	Ka	85.03	0.8285	425.76	81.12
Ti	Ka	2.24	0.0175	8.09	1.49	Ti	Ka	1.85	0.0128	5.42	1.48
Fe	Ka	8.62	0.0734	20.37	4.93	Fe	Ka	1.35	0.011	2.81	0.93

euhedral–subhedral fine- or medium-crystal dolomites. There was no direct intrusion of magma in Fengcheng Formation, and the burial depth was shallow. Scanning electron microscopy and spectroscopy data show the matrix of dolomitic rocks contains large amounts of silica and alumina ($SiO_2 + Al_2O_3$). Dolomites mainly present in subhedral fine-, powder-, or micro-crystal forms in tuffaceous or argillaceous components of the rock matrix, belonging to those formed by shallow-medium burial stage metasomatisms. In short, dolostones are mainly of shallow-medium burial type in Fengcheng Formation and partially influenced by hydrothermal fluids in the study area.

The degree of ordering is a sign for determining the crystallinity of mineral, which also reflects physical and chemical conditions in the rock-forming environment (Wenk et al., 1993; Su et al., 2011). In an early study, Goldsmith and Graff (1958) conducted X-ray diffraction analysis to investigate the ordering-disordering phenomena in dolomite crystal structure, and proposed the ratio between the intensity values of the (0 1 5) to (1 1 0) diffraction peaks, i.e., I(0 1 5)/I(1 1 0), as the degree of ordering. According to Goldsmith and Graff (1958), I(0 1 5)/I(1 1 0) = 1 indicates complete ordering in the crystal structure of dolomite; and I(0 1 5)/I(1 1 0) < 1 indicates varying degrees of disordering in the crystal structure of dolomite.

In studies on dolomitization, the degree of ordering is frequently used as one of the criteria for determining the mineral-forming (diagenetic) environment (Morrow, 1982; Andreeva et al., 2011). It is considered that dolomites formed in the syndiagenetic environment have low degrees of ordering; with increasing burial depth, the grain size of dolomites generally grows and their degree of ordering correspondingly increases. When formed in the epidiagenetic environment, dolomites can crystalize with a high degree of ordering.

Results show that the degree of order in dolostones ranges from 0.39 to 1.00 with an average of 0.63 (Table 2). The large range of variations in degree of order indicates that the dolomitization process of dolostones in the study area had been influenced by multiple factors, possibly experiencing a multi-stage process of origin.

Approximately 50% of rock samples have the degree of order in the range of 0.50–0.65 (Table 2). The relatively low range of degree of ordering reflects that Mg^{2+} ions are rich in the formation. In the X-ray diffraction analysis, dolomite crystals are mostly micritic dolomites produced by penecontemporaneous dolomitization (Table 1), and their corresponding the values of Mg/Ca ratio are relatively high. These dolomite products feature high crystallization rate, low degree of crystallinity, and low degree of ordering. It is possible that during the process of dolomitization, the joint actions of displacement cations (e.g., Fe^{2+}, Mn^{2+}, Mg^{2+}) and volcanic activities led to declines in the degree of ordering in dolomites (Liu et al., 2010).

Approximately 15% of rock samples have the degree of ordering in the range of 0.8–1.00, which coincide with relatively low molar concentrations of $CaCO_3$ (Table 2). Together the relatively high Fe^{2+} and Mn^{2+} contents in rock samples indicate that these dolostones were formed in a strongly reducing environment as the products

of displacement lime mudrock under the diagenetic condition of slow and stable crystallization, belonging to burial dolomite (FC011–1, 2; FN3–4).

5.2. Trace elements for origin

The ratio of contents between the trace elements V and Ni, i.e., V/Ni, provides a good indicator for identifying the sedimentary facies and depositional environment (Land, 1973). The V/Ni ratio is generally greater in marine sediments than in continental sediments; V/Ni < 1 indicates a marine depositional environment while V/Ni indicates a continental depositional environment; additionally, the threshold value of Ni content in sediments is 40 µg/g (Baker and Burns, 1985). In our study area, the V/Ni ratio of dolostone samples falls in the range of 1.02–4.88 > 1 with Ni content over 40 µg/g (except F18–5, 6, tuff) (Table 2). These results demonstrate that the dolostones are formed in a continental saltwater depositional environment on the northwestern margin of Junggar Basin.

Baker and Burns (1985) considered that Sr content of dolomites precipitated from normal seawater is 600 µg/g. Land (1973, 1985) proposed that Sr content of ancient dolostones rarely exceeds 200 µg/g. Yang et al. (2000) reported that Sr content of modern dolostones is 1000–1200 µg/g, that of evaporite-related hyperhaline dolostones is generally 400–550 µg/g; and that of burial dolomite is 60–170 µg/g. In our study area, the large variation range of Sr content indicates that associated dolomitization of rocks was affected by multiple factors. Approximately 11% rock samples contain 0–200 µg/g Sr, and these low levels of Sr content reflect the possible mechanism of dolostone formation via late burial diagenesis (Huang et al., 2006; Zhang, 1985) (Fig. 4). The majority of rock samples contain >400 µg/g Sr, with an average of 453.1 µg/g (Table 2). This observation reflects that dolostones were formed in a saltwater environment with high salinity and intense evaporation and possibly affected by weak interference of continental freshwater as well as the influence and transformation of structural hydrothermal fluids. Additionally, this result reflects early dolomitization. Taking into consideration of crystal fabric, we consider that this set of dolostones was related to dolomitization of high-salinity pore-water fluids in the penecontemporaneous stage.

5.3. Carbon and oxygen isotopics

C–O isotopic composition of dolomites is mainly affected by temperature and salinity in the medium (Keith and Weber, 1964a,b). In the process of diagenesis, the burial depth, temperature, and pressure increment in sediments, the leaching and dissolution of minerals through atmospheric precipitation, and associated biodegradation process pose certain influences on $\delta^{18}O_{PDB}$ and $\delta^{13}C_{PDB}$ values (Keith and Weber, 1964a,b; Wu et al., 2005). Because oxygen isotopic fractionation occurs during evaporation of water, temperature rises and intensive evaporation will lead to increases in lake water salinity and the $\delta^{18}O_{PDB}$ value (Keith

Table 2
Trace element contents and stable carbon–oxygen isotopic composition of dolomitic rocks in the study area.

Well	Sample	Lithology	MgO (%)	CaO (%)	Fe$_2$O$_3$ (%)	V (µg/g)	Ni (µg/g)	Mn (µg/g)	Sr (µg/g)	δ^{13}C$_{PDB}$ (‰)	δ^{18}O$_{PDB}$ (‰)	Degree of ordering (δ)	Mg/Ca (mol/mol)	V/Ni	Salinity index Z	Paleo temperature T(°C)
F18	F18-11	Dolomitic mudstone	5.88	6.51	2.63	63.4	28.1	747.5	533.4	4.4	1.1	0.55	1.35	2.26	136.86	8.85
F18	F18-12	Dolomitic mudstone	7.64	7.68	3.29	87.3	17.9	985.8	663.6	4.8	1.6	0.59	1.49	4.88	137.93	6.14
F18	F18-13	Dolomitic mudstone	6.1	4.46	2.86	44.7	17.9	505.9	363.2	5.1	0.9	0.66	2.05	2.5	138.19	9.93
F18	F18-14	Dolomitic mudstone	6.65	3.38	3.48	67.1	29.6	496.2	352.8	5.2	0.9	0.46	2.95	2.27	138.4	9.93
F18	F18-15	Dolomitic mudstone	1.19	2.07	3.72	87.8	36.4	529.9	209.3	3.5	−6.7	0.68	0.86	2.41	131.13	51.05
F18	F18-5	Tuffaceous dolomite	4.26	3.96	5.18	86.6	84.8	857.1	202.4	0	−13	–	1.61	1.02	120.83	85.13
F18	F18-6	Tuffaceous dolomite	4.16	4.16	5.18	77.6	99.9	883.4	178.1	−0.6	−14.8	–	1.50	–	118.7	94.87
F18	F18-7	Dolomitic mudstone	6.67	7.67	2.15	67.9	20.4	470.9	782.2	2.6	−4	0.53	1.30	3.33	130.63	36.44
F18	F18-8	Dolomitic mudstone	7.3	7.21	2.46	68.9	20.2	509	631.7	2.8	−2.8	0.65	1.52	3.41	131.64	29.95
F18	F18-9	Dolomitic mudstone	5.01	1.7	3.83	94.3	24.9	286.5	144.6	3.2	1.1	0.90	4.42	3.79	134.4	8.85
F19	F19-1	Tuffaceous dolomite	1.44	1.78	7.25	77.3		361.6	95.9	0.3	−11	–	1.21	–	122.44	74.31
FC1	FC1-1	Tuffaceous dolomite	7.66	6.19	2.76	68.1	30.3	589.2	420.7	−0.4	−0.7	0.70	1.86	2.25	126.13	18.59
FN1	FN1-10	Grey dolomitic mudstone	0.38	0.58	1.39	15.4	6.5	377.9	138.9	3.6	−3.9	–	0.98	2.37	132.73	35.9
FN1	FN1-3	Tuffaceous dolomite	5.31	8.34	2.8	48.2	22.2	592.9	598.4	−1	−0.8	0.68	0.96	2.17	124.85	19.13
FN1	FN1-4	Grey dolomitic mudstone	6.62	5.41	2.92	50.1	21.7	524.7	423.6	5	0.1	0.48	1.84	2.31	137.59	14.26
FN1	FN1-5	Grey dolomitic mudstone	2.37	2.73	3.74	61.1	28.7	499.7	222.8	4.3	−9.7	–	1.30	2.13	131.28	67.28
FN1	FN1-6	Grey dolomitic mudstone	5.36	5.88	2.58	60.6	17.1	494.9	560.5	5	−7.3	0.39	1.37	3.54	133.9	54.29
FN1	FN1-7	Grey dolomitic mudstone	5.31	4.33	2.57	46.6	32.3	441.6	420.7	4.8	−0.6	0.40	1.84	1.44	136.83	18.05
FN1	FN1-9	Grey dolomitic mudstone	7.52	6.63	3.54	73.6	22.1	888.8	593.7	4	1.9	0.75	1.70	3.33	136.44	4.52
FN2	FN2-11	Argillaceous dolomite	5.3	10.46	4.21	81.5	29.9	847.2	532.8	3.1	−6.4	0.43	0.76	2.73	130.46	49.42
FN2	FN2-5	Argillaceous dolomite	5.6	6.42	2.2	46.1	19.8	361.9	499.4	4.3	−0.8	0.57	1.31	2.33	135.71	19.13
FN2	FN2-6	Argillaceous dolomite	8.85	9.44	2.31	29.4	25.9	535.3	760.3	3.6	3.2	0.51	1.41	1.14	136.27	−2.51
FN2	FN2-7	Argillaceous dolomite	6.98	6.7	2.96	62.4	26.3	698.6	575.4	4.1	1.5	0.69	1.56	2.37	136.44	6.69
FN2	FN2-8	Argillaceous dolomite	7.9	7.71	3.41	50.6	35.1	577.8	586.1	3.5	−1.5	0.72	1.54	1.44	133.72	22.92
FN2	FN2-9	Argillaceous dolomite	8.46	8.12	3.41	74.5	22	911.5	658.6	4	0.5	0.59	1.56	3.39	135.74	12.1
FN3	FN3-10	Argillaceous dolomite	7.96	8.23	2.97	51.9	16.8	784.5	534.3	3.6	1.3	0.58	1.45	3.09	135.32	7.79
FN3	FN3-11	Argillaceous dolomite	6.46	7.9	2.49	45.9	20.2	553.6	385	3.7	1.1	0.57	1.23	2.27	135.43	8.88
FN3	FN3-13	Argillaceous dolomite	3.9	5.28	2.53	40.3	34.1	668.8	783.6	3.1	2.3	0.57	1.11	1.18	134.79	2.36
FN3	FN3-14	Argillaceous dolomite	5.81	1.7	2.5	56.8	25.2	639.4	739.9	3.1	2.3	0.67	5.13	2.25	134.79	2.36
FN3	FN3-4	Silty dolomite	2.39	2.02	6.3	109	67.8	656.3	290	0.6	−10.4	1.00	1.77	1.6	123.35	71.06
FN3	FN3-5	Silty dolomite	2.66	4.45	4.03	90.2	32	723.1	281.5	1.9	−9.3	0.62	0.90	2.82	126.56	65.11
FN3	FN3-7	Argillaceous dolomite	1.59	3.5	3.04	47.7	40.1	133	265.3	1.8	−5.9	–	0.68	1.19	128.05	46.72
FC011	FC011-1	Dolomitic siltstone	6.91	5.31	3.05	44	24	338.7	600.8	2.3	−5	0.98	1.95	1.83	129.52	41.85
FC011	FC011–2	Dolomitic siltstone	4.45	4.17	2.56	50.7	24.1	455.8	376.5	2.2	−5.1	0.85	1.60	2.1	129.27	42.39

Note: $Z = 2.048 \, (\delta^{13}C + 50) + 0.498 \, (\delta^{18}O + 50)$, $T = 14.8 - 5.41 \times \delta^{18}O + 0.04/(\delta^{18}O)^2$.
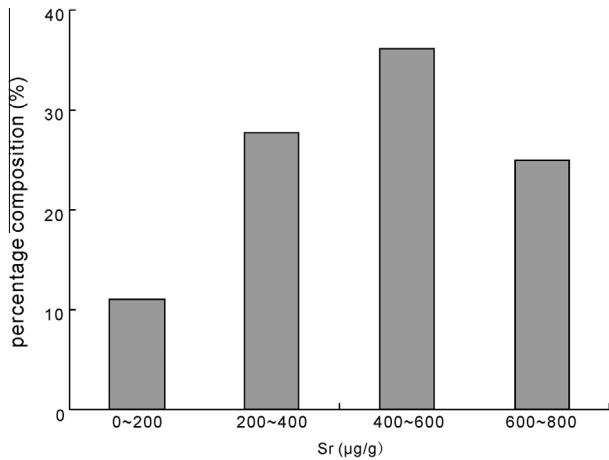
Fig. 4. The distribution of Sr abundance in dolomitic clastic rocks collected from the study area.

and Weber, 1964a,b; Li et al., 2008). C isotopic composition is influenced by different sources of carbon; thus, we can determine the source of dolomitized fluids according to different sources of carbon, further to identify the diagenetic environment (Keith and Weber, 1964a,b). Overall, the $\delta^{18}O_{PDB}$ and $\delta^{13}C_{PDB}$ values become greater with increasing salinity, and $\delta^{18}O_{PDB}$ becomes lighter with rising temperature. In the process of diagenesis, both freshwater leaching and biodegradation can make $\delta^{18}O_{PDB}$ and $\delta^{13}C_{PDB}$ lighter. On the basis of predecessors' research, we can draw a conclusion that the C–O isotope influence factors are various. In the study area. The large ranges of variations in C–O isotopic composition indicate that dolomitization occurred in different environments and via diverse mechanisms. Relatively high C–O isotope values in a narrow range ($\delta^{13}C_{PDB}$, mostly 1.5–4‰; $\delta^{18}O_{PDB}$, −1‰ to 4‰) (Fig. 5). The volcanism eruptive subfacies tuffaceous dolomite in low $\delta^{13}C_{PDB}$ (−1‰ to 0.3‰), Silty dolomite in fan-delta front subfacies sheet sand microfacies $\delta^{13}C_{PDB}$ (0.6–2.3 ‰), and, shallow, semi-deep lake subfacies $\delta^{13}C_{PDB}$ (1.8–5.2‰) (Fig. 2). All the above characteristics of dolomites are direct reflections of penecontemporaneous dolomitization. Commonly negative $\delta^{18}O_{PDB}$ values distributed in an extremely broad range (−15‰ to 0‰) indicate burial dolomitization.

Salinity index Z and paleo temperature T are two indicators for determining salinity and temperature of dolomitization using C–O isotopes (Chen et al., 2012). These two indicators are calculated as follows: $Z = 2.048 (\delta^{13}C + 50) + 0.498 (\delta^{18}O + 50)$ (Keith and Weber, 1964a,b), and $T = 14.8 - 5.41 \times \delta^{18}O + 0.04/(\delta^{18}O)^2$ (Geological Geochemistry Teaching and Research Section of Wuhan Institute, 1979). Results show that most dolostone samples (except for one case) have $Z > 120$ (Keith and Weber, 1964a,b) (Table 2). This result indicates that dolostones were formed in a high-salinity saltwater environment in the study area. Additionally, the samples have significantly varying T values in the range of −2.51 to 94.87 °C (Table 2); the large range of variations in T indicates that dolostones were formed in multi-stages. More than 60% rock samples have near-surface atmospheric temperature of 50 °C, indicating that dolomitization occurred in a penecontemporaneous evaporation environment. Those with near-surface atmospheric temperature of 50–80% account for 15% of samples, indicating that there exist burial dolomites in the study area, and the high temperature may be affected by volcanic activity and related to hydrothermal activity.

In the C–O covariant diagram (Fig. 5a) (Keith and Weber, 1964a,b), the points of dolomite are mainly distributed in and around the area (M1, G2, G1). This distribution pattern indicates

that the major origin of dolostones in the study area is burial, and that the source of Mg^{2+} ions includes clay mineral transformation and hydrothermal fluids. The points distributed between the areas of mixing water and the seepage reflux may be related to the influences of evaporation and deep thermal brine. A C–O isotope-based diagram shows the mechanism of dolostone formation (Fig. 5b) (Warren, 2000). It can be seen that dolostone formation in the study area displays high consistency with typical dolostones formed in penecontemporaneous evaporation environment and burial dolostones formed in other areas of the world, which coincides with the depositional environment and structural characteristics in the depositional period of Permian dolomitic rocks on Junggar's northwestern margin.

5.4. Formation model

A rich source of Mg is the primary issue for the occurrence of dolomitization. A previous study suggests that seawater or concentrated seawater is the major Mg source of dolomitization (Zhang, 1985). Through mineralogical and geochemical analyses combined with kinetic analysis of rock samples, the source of Mg for Permian dolomite formation on Junggar's northwestern margin includes high-Mg connate water in formations, Mg released from pore brine and clay minerals, and Mg brought by devitrification of volcanic glass and deep-earth magmatic hydrothermal fluids.

Because Fengcheng Formation was deposited in a semi-closed bay with relatively high salinity and pH values, the pore water and formation water of argillaceous components were rich in Mg^{2+} while the minerals Mg calcite and aragonite were inherently rich in Mg^{2+}. Additionally, the Urho-Fengcheng area is located in a fault zone, where underground Mg^{2+}-rich fluids upwelled from deep formations along faults and thus increased Mg^{2+} content of the pore water. Moreover, Junggar Basin experienced a volcanic activity period in the Permian and thus related to syndiagenesis of dolomitic rocks and tuff in the formations. Possible Magnesium sources included Magnesium ions separated from volcanic glass after devitrification and generated from Mg^{2+}-rich volcanic rocks via self transformation or fluid leaching and dissolution.

Based on the above mineral characteristics and geochemical data of dolomitic rocks combined with the evolutionary history palaeoclimate, we propose that the origin of Permian dolomitic rocks on Junggar's northwestern margin can be divided into three types, i.e., penecontemporaneous dolomitization, burial dolomitization, and hydrothermal dolomitization.

In the depositional period of Permian P_1f, volcanoes distributed in a bead-like pattern along Xiazijie-Mahu area partially separated Urho-Fengcheng area and the great Mahu lake, thus forming a semi-closed bay environment. Together the hot climate, intense evaporation, and less freshwater supply in the Permian led to the formation of high-salinity Mg^{2+}-rich brine during early diagenesis.

In order to more intuitive study lithology distribution in the study area, the author made a nearly east–west cross section (Fig. 6), which shows the dolomite distribution of different facies belt. According to the structure of dolomite crystals and geochemical properties of dolostones combined with the rock-forming environment and mechanism of dolostones as well as the characteristics of parallel well cross-sections (Fig. 6) and sedimentary facies, we established a dolomitization model in the Permian P_1f in Urho-Fengcheng area on the northwestern margin in Junggar Basin (Fig. 7). A lot of scrutinies on ancient and modern primary dolomite had been done, otherwise, many forming model about evaporation dolostones had been established, but volcanic materials often scarcely be mentioned (Preto et al., 2014; Frisia, 1994; Wenk et al., 1993). So via dolomite forming environment and sedimentary environment studies, this paper constructs delta – briny lacustrine – volcanism primary and non-primary dolomitic
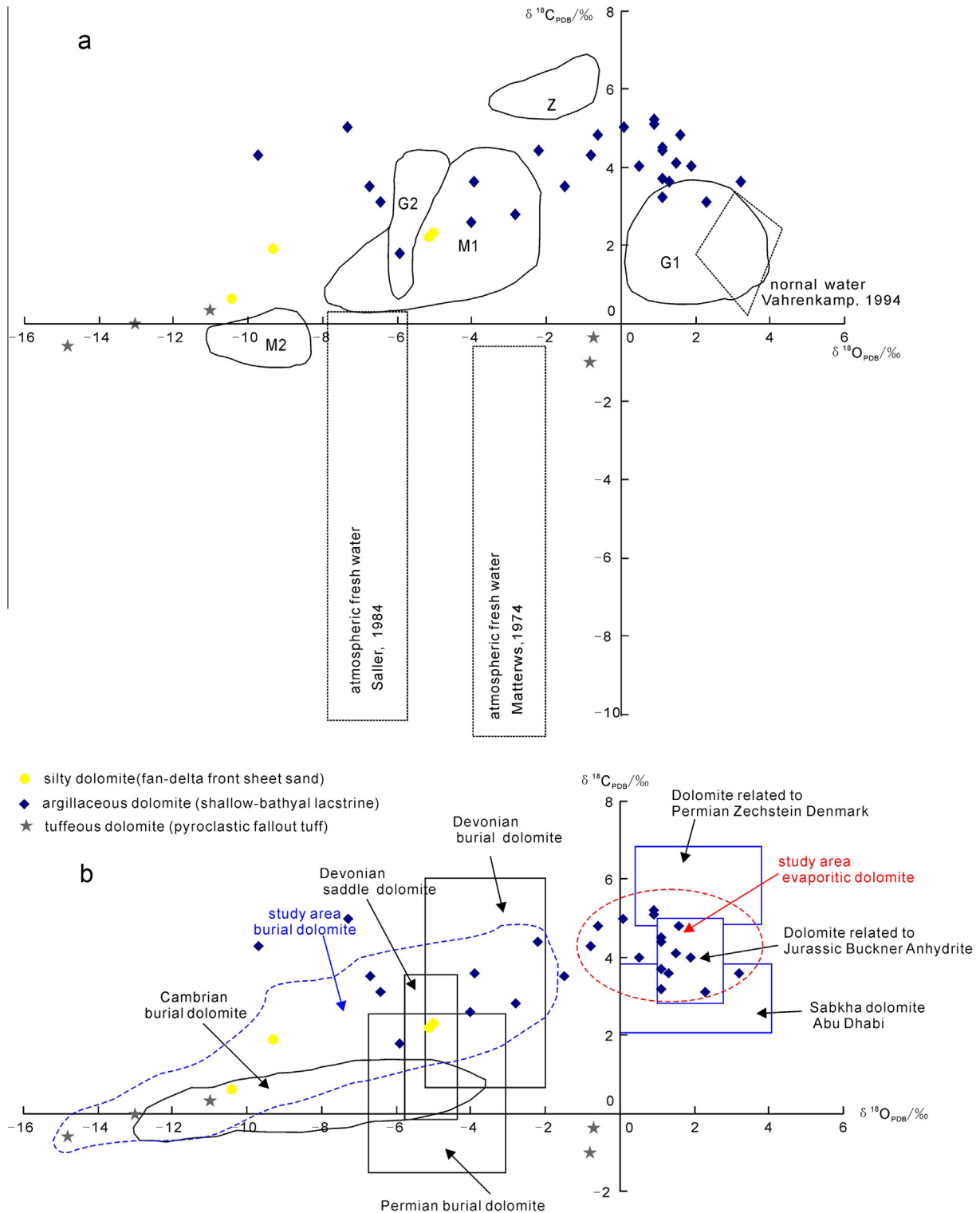
Fig. 5. Covariant diagram showing the origins of dolostones and the relationship between $\delta^{18}O_{PDB}$ and $\delta^{13}C_{PDB}$ in the study area. (a) Origins of dolostones (modified from Huang et al., 2006), Z-Seepage reflux; G1-mixing water; G2-burial ferroan dolomite; M-burial dolomite (including mudstone dehydration); M2-burial dolomite cement; normal water environment (Vahrenkamp, 1994); atmospheric freshwater(Saller, 1984; Mattews, 1974); and (b) variations in O–C isotopic composition of typical evaporation-related and burial dolostones (Warren, 2000).

model. In this model, aragonite and high-Magnesium calcite were deposited concurrently with argillaceous, silty, and tuffaceous sediments in a quiet semi-closed continental bay on the north-western margin of the basin; due to the hot climate and intense evaporation, the increasing salinity of water bodies led to penecontemporaneous dolomitization in an early stage of diagenesis; thereafter, intense tectonic activities and intermittent volcanic activities accelerated the upwelling of Mg-rich hydrothermal fluids along fault structures, leading to the formation of burial and hydrothermal dolomites in middle-late stages of diagenesis.
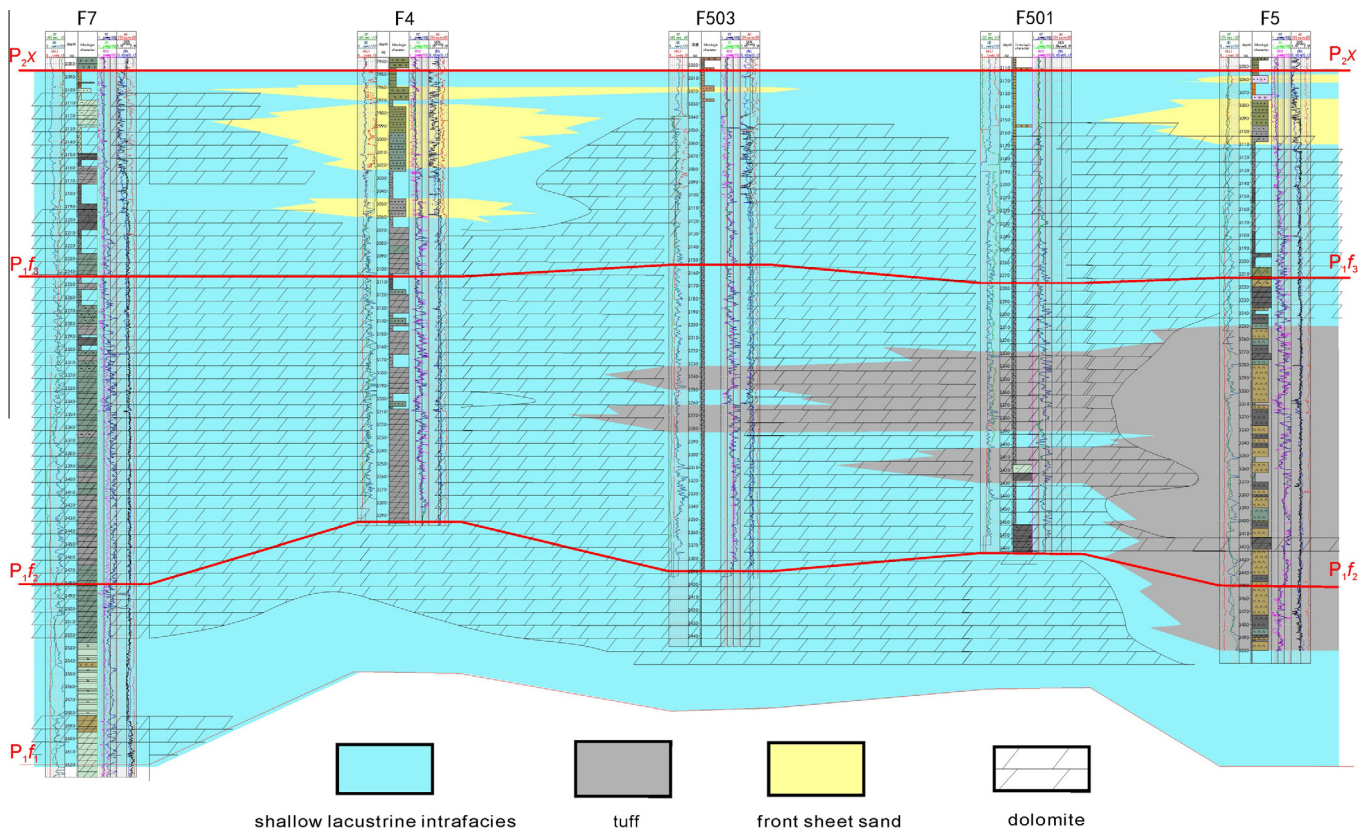
Fig. 6. A set of parallel well cross-sections (F7–F4–F503–F501–F5).
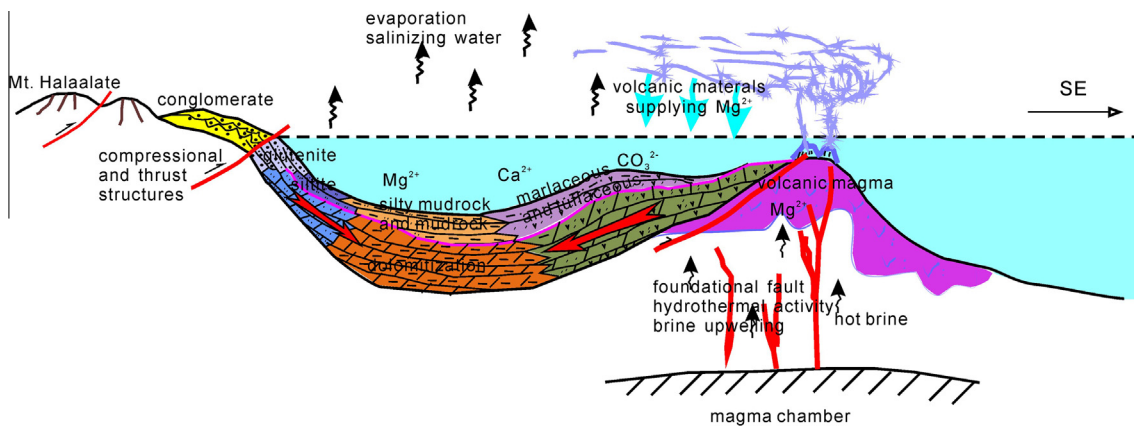
Fig. 7. A schematic diagram of the model for dolomitization in the study are.

6. Conclusions

On the northwestern margin of Junggar Basin, Permian dolomitic rocks with complex lithological characteristics mainly include dolomitic mudstone, dolomitic siltstone, dolomitized tuffaceous siltstone, and dolomitized tuffaceous mudstone. These dolomitic rocks are euhedral or subhedral fine- and medium-crystal dolomites developed along fractures and beddings, and formed by dolomitization of silty, tuffaceous, or argillaceous sediments that contained abundant tuffaceous or argilla-calcareous components and deposited a semi-closed bay environment with quite water bodies. A combination of depositional environment of dolostone formation, characteristics of rock type, differences in trace element contents, and C–O isotopic composition with geological background indicate that the Fengcheng Formation of Permian strata

in Urho-Fengcheng area, dolomitic rocks were mainly formed in a terrestrial saltwater bay. A combination of tectonic events, climatic conditions, volcanic activities, and formation water–rock reactions provided Mg-rich fluids for dolomitization and created conditions for the occurrence of metasomatism, leading to the formation of unique hydrocarbon-bearing dolostone reservoirs in the Fengcheng Formation. In the study area, dolomitic rocks have multi-stage origins involving complex mechanisms of dolomitization. Together the petrological and geochemical evidence of dolomitic rocks, complex tectonic activities of the Permian strata, associated climatic characteristics, and volcanic activities suggest that the mechanisms of dolomitization mainly include penecontemporaneous dolomitization, burial dolomitization, and hydrothermal dolomitization. It is the processes of dolomitization in different diagenetic stages and at various burial depths that

breeds the dolostone hydrocarbon reservoirs in the Permian strata on the northwestern margin of Junggar Basin.

Acknowledgements

References

Adams, J.F., Rhodes, M.L., 1960. Dolomitization by seepage refluxion. AAPG Bull. 44, 1912–1920.

Andreeva, P., Stoilov, V., Petrov, O., 2011. Application of X-ray diffraction analysis forsedimentological investigation of Middle Devonian dolomites from Northeastern Bulgaria. Geol. Balcan. 40 (1–3), 31–38.

Badiozamani, K., 1973. The Dorag dolomitization model-application to the Middle Ordovicaiafn of Wisconsin. J. Sediment. Petrol. 43, 965–984.

Baker, P.A., Burns, S.J., 1985. Occurrence and formation of dolomite in organic rich continental margin sediments. AAPG Bull. 69 (11), 1917–1930.

Baker, P.A., Kastner, M., 1981. Constraints on the formation of sedimentary dolomite. Science 213, 214–216.

Braithwaite, C.J.R., Rizzi, G., Darke, G., 2004. The Geometry and Petrogenesis of Dolomite Hydrocarbon Reservoirs. Geological Society of London Special Publication, London, vol. 235.

Chen, H.D., Hu, S.H., Chen, A.Q., Zhao, J.X., Su, Z.T., 2013. Genesis of non-karst dolomite reservoirs in the eastern central paleo-uplift in the Ordos Basin. Nat. Gas. Ind. 33 (10), 18–24.

Chen, Q., Hu, W.X., Li, Q., Zhu, J.Q., 2012. Characteristics and genesis of REE patterns of Changxing and Feixianguan dolomites in Panlongdong, northeastern Sichuan. Petrol. Geol. Exp. 33 (1), 84–93.

Dang, L.R., Zheng, R.C., Zheng, C., Wen, Q.B., Chen, S.C., Liao, J., 2011. Origis and diagenetic system of dolomite reservoirs in the Upper Permian Changxing formation, eastern Sichuan Basin. Nat. Gas. Ind. 31 (11), 47–52.

Davies, G.R., Smith Jr., L.B., 2006. Structurally controlled hydrothermal dolomites reservoir facies: an overview. Am. Assoc. Petrol. Geol. Bull. 90 (11), 1641–1690.

Fan, M.T., Yang, L.K., Fang, G.Y., Wang, M.F., Li, T.F., Zhu, L.D., 2003. Origin of lacustrine hydrothermal sedimentary rock (Lower Cretaceous) in Qingxi Sag and its significance. Acta Sedimentol. Sin. 21 (4), 560–565.

Fookes, E., 1995. Development and eustatic control of an Upper Jurassic reef complex (Saint Germain-de-Joux, eartern France). Facies 33, 129–149.

Friedman, G.M., Sanders, J.E., 1967. Origin and occurrence of dolostones. In: Chilingar, G.V., Bissell, H.J., Fairbridge, R.W. (Eds.), Carbonate Rocks: Origin, Occurrence, and Classification. Elsevier, Amsterdam, pp. 267–348.

Frisia, S., 1994. Mechanisms of complete dolomitization in a carbonate shelf: comparison between the Norian Dolomia Principale (Italy) and the Holocene of Abu Dhabi Sabkha. In: Purser, B., Tucker, M., Zenger, D. (Eds.), A Volume in Honour of Dolomieu. Int. Assoc. Sedimentol. Spec. Publ., vol. 21, pp. 55–74.

Gao, G., Land, L.S., Elmore, R.D., 1995. Multiple episodes of dolomitization in the Arbuckle Group, Arbuckle Mountains, south-central Oklahoma; field, petrographic, and geochemical evidence. J. Sediment. Res., Sect. A 65 (2), 321–331.

Gao, G., Land, L.S., Folk, R.L., 1992. Meteoric modification of early dolomite and late dolomitization by basinal fluids, upper Arbuckle Group, Slick Hills, Southwestern Oklahoma. Am. Assoc. Petrol. Geol. Bull. 76, 1649–1664.

Geng, C.Y., Chen, B.K., 2002. Subtle traps in the northwest margin of Junggar Basin. J. Chengdu Univ. Technol. 29 (2), 168–172.

Geological Geochemistry Teaching and Research Section of Wuhan Institute, 1979. Geochemistry. Science Press, Beijing.

Goldsmith, J.R., Graff, D.R., 1958. Structural and compositional variations in some natural dolomites. J. Geol. 66, 678–693.

Gunatilaka, A., Saleh, A., Al-Temeemi, A., Nassar, N., 1987. Calcium-poor dolomite from the sabkhas of Kuwait. Sedimentology 34, 999–1006.

Guo, J.G., Zhao, X.L., Liu, W., Huang, L.L., Lu, Y., Li, H., Fang, L.H., 2009. Origin and distribution of dolomite reservoir of permian fengcheng formation in Wuerhe area, Junggar Basin. Xinjiang Petrol. Geol. 30 (6), 699–701.

Hanshow, B.B., Back, W., Deike, R.G., 1971. A geochemical hypothesis of dolomitization by ground water. Econ. Geol. 66, 710–724.

He, Z.X., Zheng, C.B., Wang, C.L., Huang, D.J., 2005. Cases of discovery and exploration of marine fields in China (Part 2): Jingbian Gas Field, Ordos Basin. Mar. Origin Petrol. Geol. 10 (2), 37–44.

Hsu, K.J., Schneider, J., 1973. Progress report on dolomitization-hydrology of Abu Dhabi Sabkhas, Arabian Gulf. In: Purser, B.H. (Ed.), The Persian Gulf. Springer, New York, pp. 409–422.

Huang, C.G., Huang, S.K., Wu, S.J., Chen, Q.L., 2006. Sr-isotope composition and evolvement in sea water over past 100 Ma and control factors. J. Earth Sci. Environ. 28 (2), 19–24.

Jiang, Y.Q., Wen, H.G., Qi, L.Q., Zhang, X.X., Li, Y., 2012. Salt minerals and their genesis of the Permian Fengcheng formation in Urho area, Junggar basin. J. Miner. Petrol. 32 (2), 105–114.

Keith, M.L., Weber, J.N., 1964a. Carbon and oxygen isotopic composition of selected limestone and fossils. Geochim. Cosmoehim. Acta 28, 1787–1816.

Keith, M.L., Weber, J.N., 1964b. Carbon and oxygen isotopic composition of selected limestones and fossils. Geochim. Cosmochim. Acta 28, 1786–1816.

Kuang, L.C., Tang, Y., Lei, D.W., Chang, Q.S., Ouyang, M., Hou, L.H., Liu, D.G., 2012. Formation conditions and exploration potential of tight oil in the Permian saline lacustrine dolomitic rock, Junggar Basin, NW China. Petrol. Expl. Develop. 39 (6), 657–667.

Land, L.S., 1985. Dolomitization. Petroleum Industry Press, Beijing, pp. 1–12.

Land, L.S., 1973. Contemporaneous dolomitization of middle Pleistocene Reefs by Meteoric Water, North Jamaica. Bull. Mar. Sci. (Coral Reef Project Papers in Memory of Dr. Thomas F. Goreau) 23 (1), 64–92, 4.

Li, H., Liu, Y.Q., 2013. "Dolomite problem" and research of ancient lacustrine dolostones. Acta Sedimentol. Sin. 31 (2), 302–314.

Li, P.C., Chen, G.H., Zeng, Q.S., Yi, J., Hu, G., 2011. Genesis of Lower Ordovician dolomite in central Tarim basin. Acta Sedimentol. Sin. 29 (5), 842–856.

Li, Y.L., Huang, Y.J., Wang, C.S., Zhu, L.D., Wang, L.C., Wei, Y.S., 2008. Geochemical characteristics and genetic analysis of the Cretaceous dolomite in the Cuoqin Basin, Qing. Acta Petrol. Sin. 24 (3), 609–615.

Liu, C., Zhang, H.L., Zhang, R.H., Ren, K.X., Li, C., Chen, G., Wang, B., 2010. Geochemistry characteristic and origin of Paleogene dolomite in Kuqa Depression, Tarim Basin. Acta Sedimentol. Sin. 28 (3), 518–524.

Liu, W.B., 1989. Study on sedimentary environment of Fengcheng Formation at northweat margin of Junggar basin. Acta Sedimentol. Sin. 7 (1), 61–68.

Luo, P., Wang, S., Li, P.W., Song, J.M., Jin, T.F., Wang, G.Q., Yang, S.S., 2013. Review and prospectives of microbial carbonate reservoirs. Acta Sedimentol. Sin. 31 (5), 807–823.

Luo, Z.L., Liu, S., Xu, S.Q., 1998. Selection of favorable area of exploration in Sinian bearing gas formation of Sichuan basin. Acta Petrol. Sin. 19 (4), 1–7.

Ma, Y.S., 1999. Sedimentology of Carbonatite Reservoirs. Geology Press, Beijing.

Machel, H.G., 2004. Concepts and models of dolomitization: a critical reappraisal. In: Braithwaite, C.J.R., Rizzi, G., Darke, G. (Eds.), The Geometry and Petrogenesis of Dolomite Hydrocarbon Reservoirs. Geological Society, Special Publication, London, vol. 235, pp. 7–63.

Mattews, R.K., 1974. A process approach to diagenesis of reef-associated limestones. In: Lapovte, L.F. (Ed.), Reefs in Time and Space. SEPM Special Publication, Tulsa, vol. 18, pp. 234–256.

Morrow, D.W., 1982. Diagenesis 2. Dolomite – Part 2. Dolomitization models and ancient Dolostones. Geosci. Canada 9, 5–13.

Muchez, P., Viaene, W., 1994. Dolomitization caused by water circulation near the mixing zone: an example from the Lower Viséan of the Campine basin (northern Belgium). In: Dolomites A Volume in Honour of Dolomieu. Spec Publ. Int. Assoc. Sedimentologists. Blackwell, Oxford, vol. 21, pp. 155–165.

Preto, N., Breda, A., Corso, J. D., Spotl, C., Zorzi, F., Frisia, S., 2014. Primary dolomite in the Late Triassic Travenanzes Formation, dolomites, Northern Italy: facies control and possible bacterial influence. Sedimentology. doi: http://dx.doi.org/10.1111/sed.12157.

Qi, X.F., Wu, X.Z., 2009. Depositional Environment of Paleogene Anjihaihe Formation in Southern Margin of Junggar Basin and Its Significance in Petroleum Geology. Xinjiang Petrol. Geol. 30 (3), 289–292.

Qing, H., Mountjoy, E.W., 1994a. Formation of coarsely crystalline, hydrothermal dolomite reservoirs in the Presquile Barrier, Western Canada Sedimentary Basin. Am. Assoc. Petrol. Geol. Bull. 78 (1), 55–77.

Qing, H.U., Mountjoy, E.W., 1994b. Rare earth element geochemistry of dolomites in the Middle Devonian Presqu'ile barrier, Western Canada Sedimentary Basin: implications for fluid-rock ratios during dolomitization. Sedimentology 41 (4), 787–804.

Roehl, P.O., Choquette, P.W., 1985. Carbonate Petroleum Reservoirs. Casebooks in Earth Science Series. Springer-Verlag, Berlin, Heidelberg. New York, Tokyo. (xxii + 622pp).

Sam Jr., Bogg, 2001. Principles of Sedimentology and Stratigraphy. Prentice Hall, Upper Saddle River, pp. 1–726.

Saller, A.H., 1984. Petrologic and geochemical constraints on the origin of subsurface dolomite, Enewetak At-oll: an example of dolomitization by normal sea water. Geology 12, 217–220.

Su, Z.T., Chen, H.D., Xu, F.Y., Wei, L.B., Li, J., 2011. Geochemistry and dolomitization mechanism of Majiagou dolomites in Ordovician, Ordos, China. Acta Petrol. Sin. 27 (8), 2230–2238.

Tian, J.C., Zeng, Y.F., Zheng, H.R., Kong, F.X., Feng, Y.L., 2000. The research of the reservoir characteristics of the dolostone intercalated in mudstone in terrigenous oil-bearing basin – taking the dolostone on the upper of Sha3 in Dongying sag as an example. J. Chengdu Univ. Technol. 27 (1), 88–91.

Vahrenkamp, V.C., Swart, P.K., 1994. Late Cenozoic dolomites of the Bahamas: metastable analogues for the genesis of ancient platform dolomites. In: Purser, B., Tucker, M., Zenger, D. (Eds.), Dolomites. International Association of Sedimentologists Special Publication, vol. 21, pp. 133–153.

Wachter, E., Hayes, J.M., 1985. Exchange of oxygen isotopes in carbon-dioxide phosphoric acid systems. Chem. Geol. 52, 365–374.

Wang, D., Chen, D.Z., Yang, C.C., Wang, X., Wu, M.B., Xing, X.J., 2010. Classification of texture in burial dolomite. Acta Sedimentol. Sin. 28 (1), 17–25.

Warren, J.K., 1999. Evaporites: Their Evolution and Economics. Blackwell Scientific Publications, Oxford, pp. 1–438.

Warren, J., 2000. Dolomite: occurrence, evolution and economically important associations. Earth Sci. Rev. 52, 1–81.

Wenk, H.R., Meisheng, H., Frisia, S., 1993. Partially disordered dolomite: microstructural characterization of Abu Dhabi sabkha carbonates. Am. Mineral. 78, 769–774.

Weyl, P.K., 1960. Porosity through dolomitization: conservation of mass requirements. J. Sediment. Petrol. 30 (1), 85–89.

Wu, S.J., Huang, S.J., Sun, Z.L., Hu, Z.W., Pei, C.R., 2005. Dolomite cement and its formation mechanism in the Triassic Yanchang sandstone, Ordos Basin, China. J. Chengdu Univ. Technol. (Nat. Sci. Ed.) 32 (6), 569–575.

Xue, J.J., Sun, J., Zhu, X.M., Liu, W., Zhu, S.F., 2012. Characteristics and formation mechanism for dolomte reservoi of Permian Fengcheng Formation in Junggar Basin. Geosci. 26 (4), 55–63.

Yang, W., Wang, Q.H., Liu, X.C., 2000. Dolomite origin of Lower Ordovician in Hetian River Gas Field, Tarim Basin. Acta Sedimentol. Sin. 18 (4), 544–547.

Yang, Y., Zha, M., 2007. Development of unconformity and its effect on the migration and accumulation of hydrocarbon in Wu'erhe-Xiazijie area, Junggar Basin. Petrol. Expl. Develop. 34 (3), 304–309.

Zenger, D.H., Dunham, J.B., Ethington, R.L., 1980. Concepts and Models of Dolomitization. SEPM Special Publications, Tulsa, vol. 28, p. 1–328.

Zhang, J.J., Huang, P., Feng, X.Q., Yang, D.M., Zhang, Z.H., 2011. Analysis of reservoir space characteristics of dolomite reservoirs in Sha 1 lower sub-interval in Qikou Depression. Sci. Technol. Rev. 29 (17), 39–43.

Zhang, L.G., 1985. Application of the Stable Isotope to Geology. Shaanxi Science and Technology Press, Xi'an, pp. 1–266.

Zhang, X.F., Hu, W.X., Zhang, J.T., Wang, X.L., Xie, X.M., 2008. Geochemical analyses on dolomitizing fluids of Lower Ordovician carbonate reservoir, Tarim basin. Earth Sci. Front. 15 (2), 080–089.

Zhang, X.B., 1993. Study on the origin of the dolostone intercalated in the black shales in Middle Permian Lucaogou Formation eastern part of southern margin of Junggar Basin. Acta Sedimentol. Sin. 11 (2), 132–138.

Zhang, Y.J., Qi, X.F., Cheng, X.S., Luo, Z.J., 2007. Approach to sedimentary environment of Late Carboniferous-Permian in Junggar basin. Xinjiang Petrol. Geol. 28 (6), 673–675.

Zheng, R.C., Hu, Z.G., Feng, Q.P., Zheng, C., Luo, P., Chen, S.C., 2007. Genesis of dolomite reservoir of the Changxing formation of Upper Permian, Northeast Sichuan basin. J. Miner. Petrol. 27 (4), 78–84.

Zhu, S.F., Zhu, X.M., Tao, W.F., Liu, S.Q., Chen, H.H., Zhang, Y.Q., 2013. Origin of dolomitic reservoir rock in the Permian Fengcheng formationin Wu-Xia area of the Junggar basin. Geol. J. China Univ. 19 (1), 38–45.